The Effects of Acrylate Monomers and Polystyrene Addition on the Morphology of DOP-Plasticized Styrene–Acrylate Polymer Particles Prepared by SPG Emulsification and Suspension Polymerization

Roongkan Nuisin,[1] Shinzo Omi,[2] Suda Kiatkamjornwong[3]

[1]*Department of General Science, Faculty of Science, Chulalongkorn University, Bangkok 10330, Thailand*
[2]*Graduate School of Bio-Applications and Systems Engineering, Tokyo University of Agriculture and Technology, Tokyo 184-8588, Japan*

Received 27 December 2004; accepted 28 March 2005
DOI 10.1002/app.22595
Published online in Wiley InterScience (www.interscience.wiley.com).

ABSTRACT: Fairly uniform copolymer particles of methyl acrylate (MA), butyl acrylate (BA), or butyl methacrylate (BMA) were synthesized via Shirasu porous glass (SPG) membrane and followed by suspension polymerization. After a single-step SPG emulsification, the emulsion composed mainly of the monomers. Hydrophobic additives of dioctyl phthalate (DOP), polystyrene molecules, and an oil-soluble initiator, suspended in an aqueous phase containing poly(vinyl alcohol) (PVA) stabilizer and sodium nitrite inhibitor ($NaNO_2$), were subsequently subjected to suspension polymerization. Two-phase copolymers with a soft phase and a hard phase were obtained. The composite particles of poly(St-*co*-MA)/PSt were prepared by varying the St/PSt ratios or the DOP amount. The addition of PSt induced a high viscosity at the dispersion phase. The molecular weight slightly increased with increasing St/PSt concentration. The multiple-phase separation of the St-rich phase and PMA domains, observed by transmission electron microscopy, was caused by composition drift because the MA reactivity ratio is greater than that of St. The addition of DOP revealed the greater compatibility between the hard-St and soft-MA moieties than that without DOP. The phase morphologies of poly(St-*co*-MA), poly(St-*co*-BMA), and their composites with PSt were revealed under the influence of DOP. © 2005 Wiley Periodicals, Inc. J Appl Polym Sci 99: 1195–1206, 2006

Key words: suspension polymerization; polystyrene; plasticizer; morphology; Shirasu porous glass (SPG)

INTRODUCTION

Polymer latices are a colloidal dispersion of polymer particles in a liquid, usually water. Typically, polymer lattices containing uniform polymeric particles in a submicron-size range are produced by emulsion polymerization. The shape of the particles is spherical or close to a sphere. The emulsion polymerization method for preparing monodisperse spheres has also been applied to a synthesis of nonspherical particle.[1] Monodisperse particles may be used as a flattening agent for latex paint and powder paint. They may also be used as toners, for example in xerography. Moreover, the larger sized monodisperse particles may also be used for the preparation of stationary material in gel permeation chromatography (GPC), where it is preferred that the particles are monodisperse to attain a minimum pressure drop in the column.[2,3] The core–shell polymer can be synthesized by the copolymerization of low and high glass transition polymers. Such heterogeneity can provide uniquely tailored properties, e.g., dispersion of a soft, lower glass transition temperature (T_g) latex or a soft particle core entrapped in a matrix of a harder polymer shell, which can prevent cracks in the film as an impact modifier.[4–8]

Over the past 10 years, there has been an increasing interest in the technique for making emulsions through a membrane, known as a membrane emulsification.[9–11] The Shirasu porous glass (SPG) membrane emulsification is a promising technique yielding monodisperse droplets continuously both in an oil-in-water emulsion[9–12] and a water-in-oil emulsion systems.[13,14] This method involves the use of low pressure to force the dispersed phase to permeate through a membrane, having a uniform pore-size distribution, into the continuous phase. The resulting droplet size is controlled primarily by the choice of pore size of the membrane. The technique is attractive due to its simplicity, its consumption of lower energy, and the lesser

Correspondence to: Suda Kiatkamjornwong, Program of Petrochemistry and Polymer Science, Center of Excellence for Imaging and Printing Technology, Faculty of Science, Chulalongkorn University, Bangkok 10330, Thailand (ksuda@chula.ac.th).

Contract grant sponsor: Thailand Research Fund; contact grant number: 2.M.CU/42/E.1.
Contract grant sponsor: BASE, Tokyo University of Agriculture and Technology

amount of surfactant and the narrow droplet size distribution.[11] By applying this technique, polymeric microspheres with a diameter range of about 3–100 μm have been successfully prepared by several research groups.[15–22] However, little systematic work has been reported in detail on membrane emulsification, in which plasticizers are added to many viscous liquids used as the dispersion phase.[23,24]

In our previous article,[23] we synthesized poly(St-*co*-MA) and poly(MMA-*co*-MA) in the presence of dioctyl phthalate (DOP). The comonomer pairs of poly(MMA-*co*-MA) compatibilized well with DOP than poly(St-*co*-MA). All the understudied comonomer pairs exhibited composition drift during the copolymerization because of their substantial difference in monomer reactivity ratios, which was also evidenced by the T_g values of the copolymers. In the present article, the SPG emulsification technique and subsequent suspension polymerization were used in the syntheses of poly(St-*co*-MA), poly(St-*co*-BMA), and poly(St-*co*-BA) in the presence of DOP and/or polystyrene (PSt), a bulky molecule. Effects of the added DOP plasticizer on copolymer morphology, glass transition temperature, molecular weight and particle size were investigated.

EXPERIMENTAL

Materials

Styrene (St), methyl acrylate (MA), butyl methacrylate (BMA), and butyl acrylate (BA) were of reagent grade (all from Wako Pure Chemicals, Osaka, Japan), and were distilled before use to remove the inhibitor. They were stored at −10°C prior to use. PSt, having an $\bar{M}_n$ = 4200, $\bar{M}_w$ = 40,000, and $\bar{M}_w/\bar{M}_n$ = 9.54, was prepared in-house. DOP (Fluka, Buchs, Switzerland) was used as a plasticizer. *N*,*N*′-Azobisisovaleronitrile (ADVN-V65, Wako Pure Chemicals, Osaka, Japan) or benzoyl peroxide (BPO, Kishida Chemicals, Osaka, Japan) was used as initiator. Sodium lauryl sulfate (Merck, Damstadt, Germany) and poly(vinyl alcohol) (PVA-217, Kuraray, Osaka, Japan), having 88.5% saponification and a degree of polymerization of 1700, were used as a surfactant and a stabilizer, respectively. Sodium nitrite ($NaNO_2$, Chameleon Chemicals, Osaka, Japan) and *p*-phenylenediamine (Chameleon Chemicals) were used as inhibitors. Sodium sulfate (Na_2SO_4, Kokusan Chemical Works, Osaka, Japan) was used as an electrolyte. Methyl alcohol (Kishida Chemicals, Osaka, Japan) was used as a nonsolvent for the copolymers.

Emulsification procedure

The SPG membrane (Ise Chemical Corp., Tokyo, Japan) with a pore size of 0.90 μm was used for the emulsification. The preparative conditions for a single-step emulsification and experimental results are shown in Table I.[23] Air pressure was used to permeate the dispersion phase through the SPG membrane, with ranges of pressure of 0.30–0.70 kgf cm^{-2}. The dispersion phase containing a mixture of the monomers, DOP, and BPO, or ADVN initiator was prepared. In a continuous phase, the PVA stabilizer, SDS surfactant, Na_2SO_4 electrolyte, and $NaNO_2$ inhibitor were dissolved. To prevent creaming of the droplets, the continuous phase was gently stirred at 300 rpm with a magnetic bar.

TABLE I
A Selected Recipe for the SPG Emulsification

Component	Weight (g)
Continuous phase	
PVA-217	2.00
SLS	0.10
Na_2SO_4	0.10
Inhibitor ($NaNO_2$ or PDA)	0.04
Water	230
Dispersion phase	
Initiator (BPO or ADVN)	0.04
Monomer content (St, MA, BA, BMA)	16.0
DOP	0.8

Polymerization

The monomer droplets obtained were transferred to a three-necked glass vessel with a capacity of 300 cm^3 connected with a semicircular anchor-type blade made of PTFE for agitation, a Dimorph condenser, and a nitrogen inlet. Nitrogen gas (Tokyo Chemicals Co., Tokyo, Japan) was gently bubbled into the emulsion for 1 h; the nozzle was then lifted above the emulsion level. The temperature, controlled in a thermostat bath with heating coil and circulation pump (Yamato BM-82, Tokyo, Japan), was increased to reach 75°C, and the emulsion was polymerized for 24 h in a nitrogen atmosphere by suspension polymerization.

Characterization

Conversion of monomers

The percentage conversion of the monomer was monitored by gravimetric method. Methyl alcohol was added to precipitate the polymer. The polymer particles were separated by centrifugation at 2000 rpm, and were washed repeatedly 2–3 times with methyl alcohol. The polymer particles were dried in vacuum at room temperature for 48 h and were then weighed.

Internal morphology

The internal morphologies of polymer particles in Runs 2018 and 2019 prepared from St:MA contents of

50 : 50, and 75 : 25, with an incorporation of 5% DOP, were observed by TEM (Model JEM 1010, JEOL, Tokyo, Japan). The samples were characterized for internal morphology (Act Research Co. Ltd., Yokkaichi, Tokyo, Japan). The specimens were prepared by embedding them in an epoxy resin and curing them at ambient temperature for 8 h. The samples were microtomed and stained with RuO_4, and were viewed at a magnification of 20,000×.

The internal morphology of the other polymer particles was also observed by TEM (Model JEM 200cx, JEOL-USA, Inc., Massachusetts). The specimens were prepared by embedding the polymer sample in an epoxy resin. The embedded specimens were cured at room temperature for 72 h, and were cut into thin sections of 50 nm using an ultramicrotome. Then, the ultrathin cross-sectioned specimens were stained by exposing to OsO_4 vapor from the 0.5% OsO_4 solution for 3 h prior to the TEM investigation.

Size and size distribution of emulsion droplets and polymer particles

Monomer droplets before polymerization were observed by optical microscopy (OM; Olympus BHC optical microscope, Tokyo, Japan). Diameters of about 150 monomer droplets were measured to calculate an average diameter and size distribution. The diameters of the polymer particles were obtained by the SEM techniques.

On average, the diameters of 200 polymer particles were determined from SEM (JEOL, Model JSM-5310, Tokyo, Japan). Through the evaluation of the OM and SEM photographs, the number-average diameters of the emulsion droplets (D_e) and polymer particles (D_p) were then calculated according to eq. (1), while the standard deviation (σ) and coefficient of variation (CV) were calculated using the formula in eqs. (2), (3):

$$\bar{D}_n = \sum_{i=1}^{n} n_i D_i / \sum_{i=1}^{n} n_i \quad (1)$$

where n_i is the number of particle diameter, D_i is the individual particle diameter, and $\bar{D}_n$ corresponds to the mean diameter of the particle population. The standard deviation σ is determined from the measured particle diameters as in the following equation:

$$\sigma = \left[\frac{1}{N-1} \sum_{i=1}^{N} (D_i - \bar{D}_n)^2 \right]^{1/2} \quad (2)$$

The particle size distribution is reflected in the standard deviation. The breadth of the particle size distribution is proportional to the standard deviation of the particle diameters, using the CV as follows:

$$CV\ (\%) = \sigma / \bar{D}_n \times 100 \quad (3)$$

Molecular weights and distribution

GPC (Tosoh HLCH 820, Tosoh Corp., Tokyo, Japan) was used for the examination of average molecular weights and molecular weight distribution. The GPC chromatograms were obtained using Tosoh GPC (model HLCH820 Chromato column) at an oven temperature of 40°C and an injection temperature of 35°C. Pressure was applied to the samples at 16 kgf cm^{-2}, and the reference at 12 kgf cm^{-2}. There were two types of GPC columns for sample analysis. The first column (model GRCX4 Chromato column) and the second column (model GMMXL Chromato column) were both packed with mixed gels of poly[(divinyl benzene)-*co*-styrene]. Likewise, the reference column (model GMMXL Chromato column) was also packed with mixed gels of poly[(divinyl benzene)-*co*-styrene]. Tetrahydrofuran (THF; Kishida Chemicals, Osaka, Japan) was used as a solvent and an eluent. For analysis, 1 mg of the dried polymer sample was dissolved into 2 ml of THF to obtain an approximate concentration of 0.1 wt %. Then, the polymer solution was filtered with 0.2 μm PTFE membrane (Advantec Co., Ltd, Kyoto, Japan), and was injected into the columns at a flow rate of 0.5 cm^3 min^{-1}. The chromatogram was detected by a refractive index detector.

Glass transition temperature

Measurements of glass transition temperature (T_g) of the polymer particles were performed using a differential scanning calorimeter (model 3100, MAC Science, Tokyo, Japan). The samples used were the unclean or clean particles. For the first set of unclean polymer, the polymer latex was dried under vacuum at ambient temperature for 120 h without further cleaning. For the second set, the polymer latex was washed repeatedly with methanol to remove all the surfactant and stabilizer. Then, the precipitated latex was dried under vacuum at ambient temperature for 48 h. The sample (5–10 mg) from each set was placed in an aluminum pan and put on the sensor at room temperature along with an empty pan as the reference to adjust output balance. Measurement was done at a heating rate of 10°C min^{-1} from –30°C to 130°C.

RESULTS AND DISCUSSION

Internal morphology of poly(St-*co*-MA)

The microtomed and stained polymer particles (Runs 2018 and 2019 shown in Table II) reveal their internal morphology as shown in Figure 1. The particles were stained with RuO_4 vapor (Runs 2018 and 2019) to ensure an adequate contrast between PSt and PMA

TABLE 2
Recipe and Results of Styrene and Methyl crylate Copolymerization[23]

Run No.	Composition	Monomer Composition (wt %)	Monomer Conversion (%)	D_e (μm)	CV_e (%)	D_p (μm)	CV_p (%)	$\bar{M}_n$ ($\times 10^{-4}$)	$\bar{M}_w$ ($\times 10^{-4}$)	PDI	T_g(°C)clean	T_g (°C) unclean
2018	P(St-*co*-MA)	50/50	22.37	6.1	14.7	4.8	15.6	2.0	6.3	3.2	13.4/64.1[a]	12.8/41.9[a]
2019	P(St-*co*-MA)	75/25	49.71	4.9	20.6	4.4	26.5	2.4	19.0	7.8	6.0/67.5[a]	3.7/33.6[a]
2022	P(St-*co*-MA)	50/50	93.0	8.4	21.6	3.8	13.1[b]	2.0	4.4	2.2	23.2/65.4[a]	17.5/37.9[a]
2023	P(St-*co*-MA)	75/25	89.7	5.8	10.0	4.8	10.8	1.6	3.9	2.4	11.2/78.2[a]	11.0/47.5[a]
2046	P(St-*co*-MA)/DOP	52/48	17.4	6.5	15.3	5.8	16.5	0.4	1.6	4.5	21.1/55.1[a]	23.1
2028	P(St-*co*-MA)/DOP	75/25	52.2	7.1	16.1	5.9	19.7	1.6	3.6	2.3	24.9/58.3[a]	22.0/60.3[a]
2024	P(St-*co*-MA)/PSt	37.5/50/12.5	89.8	7.8	21.1	5.2	15.8	1.3	3.8	2.8	26.7/72.2[a]	25.4/50.4[a]
2025	P(St-*co*-MA)/PSt	62.5/25/12.5	69.6	6.1	10.4	4.4	14.3	1.5	3.2	2.2	31.7/53.9[a]	20.9/49.9[a]
2029	[P(St-*co*-MA)/PSt]/DOP	37.5/50/12.5	38.9	7.0	16.1	5.0	18.3	1.2	3.2	2.8	22.2/50.1[a]	22.9/44.2[a]
2030	[P(St-*co*-MA)/PSt]/DOP	62.5/25/12.5	67.5	5.9	10.1	4.1	13.8	1.5	3.9	2.6	15.0/51.7[a]	14.6/46.9[a]

SPG membrane pore size of 0.90 μm.
[a] Two separated T_g values were observed.
[b] Coagulated particles were partially observed.

Figure 1 TEM photographs of microtomed, RuO_4-stained poly(St-*co*-MA) particles: (a) St : MA 50 : 50 (Run 2018), and (b) St : MA 75 : 25 (Run 2019).[23]

phases. The internal particle morphology was observed in various monomer compositions. The TEM photographs of poly(St-*co*-MA) with St : MA of 50 : 50 and 75 : 25 are shown in Figure 1(a,b). On viewing the inside of the particles, the minute white granules rich in MA were revealed. These granules were not found at the outermost submicron thickness or at the circumference of the particles. When a higher concentration of styrene was incorporated, larger sizes of the minute white granules were produced as shown in Figure 1(b).

When the droplets are formed, there is a time lapse before the subsequent suspension polymerization to take place. We observed a separation of some droplets suspended or dispersed inside the large drops. Because of the different reactivity ratios of the two

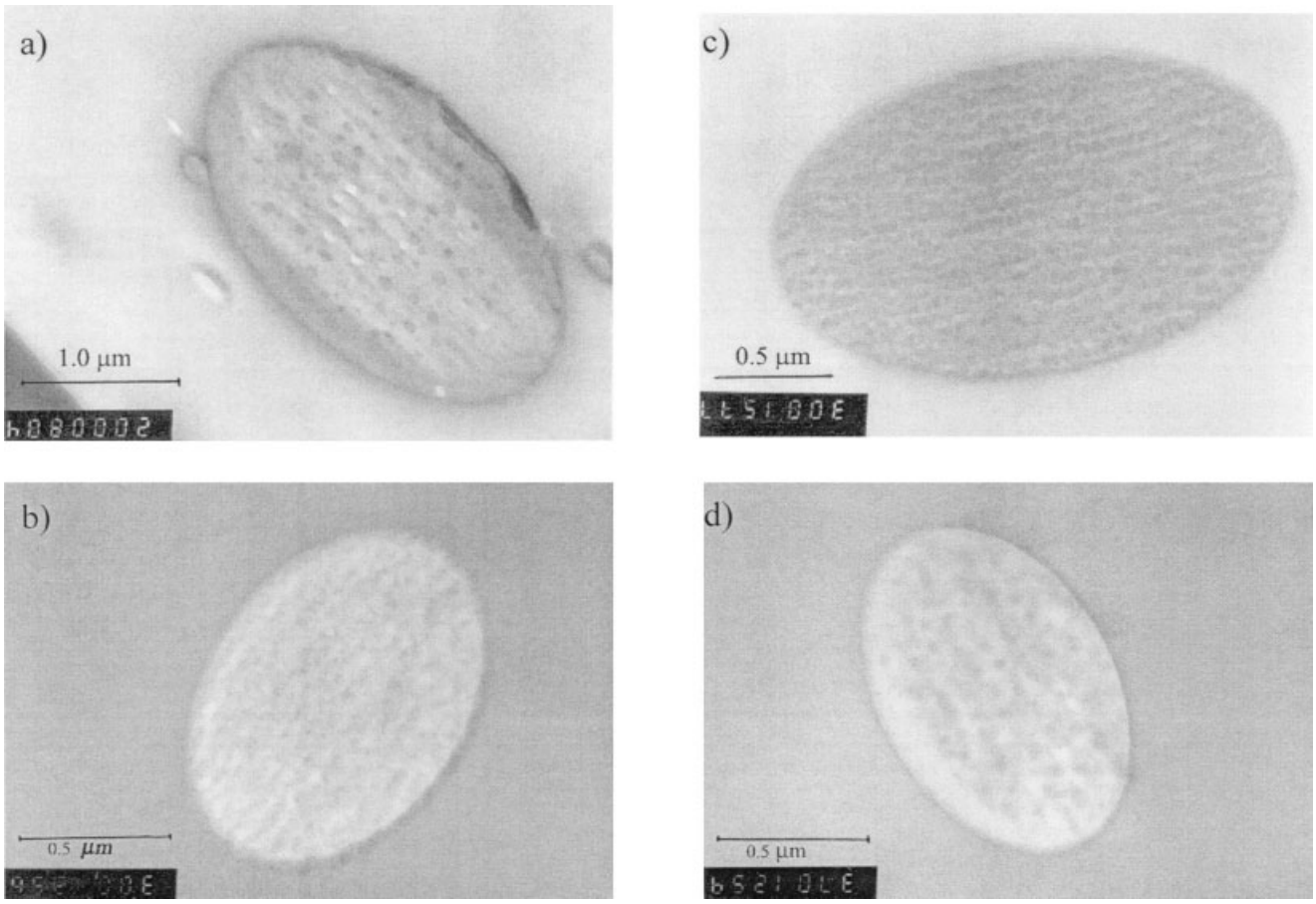

Figure 2 TEM photographs of microtomed, OsO_4-stained poly(St-*co*-MA)/PSt composite polymer particles: (a) St : MA : PSt 37.5 : 50 : 12.5 (without DOP, Run 2024), (b) St : MA : PSt 37.5 : 50 : 12.5 (with DOP, Run 2029), (c) St : MA : PSt 62.5 : 25 : 12.5 (without DOP, Run 2025), and (d) St : MA : PSt 62.5 : 25 : 12.5 (with DOP, Run 2030).

monomers, r_1(St) = 0.192 and r_2(MA) = 0.80,[25] MA monomers were consumed faster at the beginning of the polymerization to form MA-rich copolymers, which later grew to the small domains. The styrene-rich phase was subsequently produced, which later became the matrix for the MA domains because of its higher fraction in the monomer mixture. The TEM photographs also suggested that some diffusion of MA-rich domains into the St-rich polymer matrix probably took place.

Poly(St-*co*-MA)/PSt composite

To investigate the effect of the inert polymer chains dissolved in the monomer phase on the final particle morphology, PSt ($\bar{M}_n$ = 4200, $\bar{M}_w$ = 40,000, and $\bar{M}_w/\bar{M}_n$ = 9.54) was dissolved in the oil phase or the mixture of styrene and MA monomers, and the polymerization was then carried out as mentioned earlier. The formulation along with the result for each run is shown in Table II.[23] The poly(St-*co*-MA) particles were stained by OsO_4 vapor. The acrylic phase can also be stained with OsO_4. Schulze et al.[26] stained polymethacrylates in the presence of polyethylene to study the morphology of a number of materials. PSt has only the aromatic conjugated double bonds and thus will not be stained with OsO_4. Polyalkyl (meth)acrylate has regular aliphatic double bonds so it can be stained easily with OsO_4. However, Vitali and Montani[27] pointed out that the low diffusion of OsO_4 often results in a poor contrast between the phases leading to less precise determinations.

Poly(St-*co*-MA)/PSt particles exhibited a normally obtained internal morphology. The darkly-stained granules were rich in PMA and grew inside because the MA reactivity ratio is greater than that of styrene, MA monomers were thus consumed faster at the beginning of the polymerization to form the small domains. The styrene-rich phase was subsequently produced, and later became the matrix for the MA domains. The compatibility between PSt and the newly formed poly(St-*co*-MA) became less favorable because of the decreasing fraction of styrene in the copolymer chains as shown in Figure 2(a). Then, 5 wt % DOP based on monomer was added when the proportion of St:PSt was higher, in Run 2025 in Table II. It was found

that the PSt contents were less compatible with PMA and provided the core–shell-type morphology, the phase-separated domains of PMA remained in the particles as shown in Figure 2(c). One can see that the thin shell of PSt hard phase covers the soft phase of particles almost completely. The preferential staining led to differences in contrast, indicated by the dark and tiny granules of MA-rich region in the inner part of the particles. The addition of DOP plasticizer led to difference in contrast of the dark-gray PMA and light-gray PS (the lower contrast). Also, the thin shell of hard PS was observed as shown in Figure 2(b,d). Comparison with the copolymer of poly(St-*co*-MA) without the addition of PSt indicated the different types of particle morphology. As shown in Figure 3(a–c), the core–shell-type morphology is observed although the shell is difficult to be recognized. Since the reactivity ratio of MA is greater than that of styrene, MA monomer domains were generated faster at the beginning of the polymerization. Then, the St-rich phase was subsequently formed, which covered the MA-rich domains. For the St : MA ratio of 75 : 25, the phase separation is more obvious as shown in Figure 3(b). DOP limited an extent of compatibility with St-rich or PSt phase and promoted the formation of hydrophobic domains migrating to the surface resulting in core/shell morphology. The addition of DOP revealed the better compatibility between the hard-St and soft-MA phases, the dark-gray and light-gray regions were then observed. This implies that the addition of DOP may play a role of compatibilizer, and promotes the occurrence of phase behavior in polymer blends. Also, without the use of DOP, as shown in Figure 1(a,b), salami-like morphologies were favored.

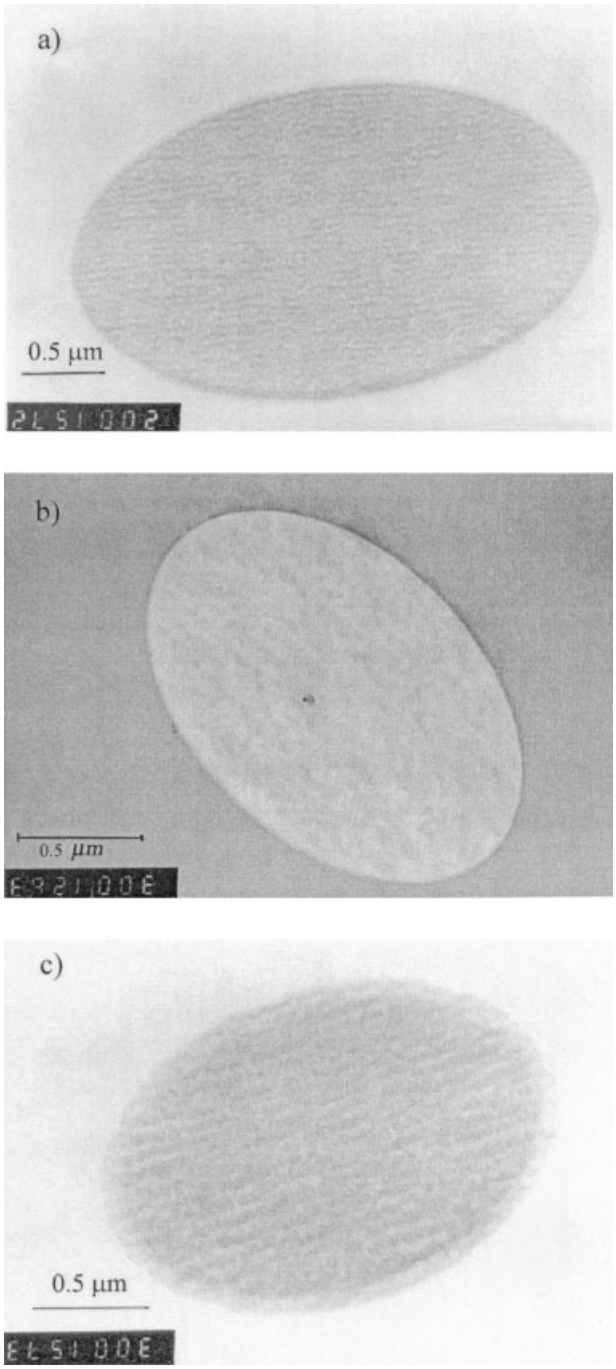

Figure 3 TEM photographs of microtomed, OsO_4-stained poly(St-*co*-MA) copolymer particles: (a) St : MA 50 : 50 (without DOP, Run 2022), (b) St : MA 50 : 50 (with DOP, Run 2046), and (c) St : MA 75 : 25 (without DOP, Run 2023).

Effect of addition of PSt on phase properties of poly(St-*co*-BMA) copolymer

The SPG membrane pore size of 0.90 μm was used for the emulsification of St and BMA, and the results are shown in Table III. The amount of the BMA phase was varied from 20 to 50 wt % in the monomer mixture in the presence of 5 wt % DOP of total monomer mixture. When the BMA phase is higher than 50 wt %, the particles become flattened, which is in agreement with our previous work.[22] The spherical particles having smooth surface were synthesized and found without a phase separation. Upon an addition of 12.5 wt % PSt into the St–BMA mixture, viscosity of the dispersion phase significantly increased. The number-average molecular weight of the resulting copolymer was close to 5000, as shown in Table III (Runs 2051 and 2052). We anticipate that PSt added functions as if it were a macromonomer (a bulky type), which diffuses rather slowly in the monomer mixture. Thus, since it is of rather high molecular weight, the addition of PSt retards the propagation step of St and BMA monomers. Therefore, the higher molecular weight PSt can be considered as somewhat of a kind of molecular spacer to prevent the propagating radicals from adding more monomers. The possible chance for these short propagating radicals is to terminate, which ultimately results in the lower average molecular weight.[24]

One possibility drawn on particle morphology prediction can be proposed as shown in Figure 4. Two

TABLE 3
Styrene and BMA Copolymerization Recipe and Results

Run No.	Composition	Monomer composition (wt %)	Monomer conversion (%)	D_e (μm)	CV_e (%)	D_p (μm)	CV_p (%)	$\bar{M}_n$ ($\times 10^{-4}$)	$\bar{M}_w$ ($\times 10^{-4}$)	PDI	T_g (°C) clean	T_g (°C) unclean
2054	P(St-*co*-BMA)	75/75	70.1	7.5	12.1	6.3	13.0	1.3	5.6	4.2	13.0/62.2[a]	22.2/94.3[a]
2059	P(St-*co*-BMA)/DOP	75/25	83.1	10.4	17.9	7.3	22.0	2.7	6.1	2.2	22.5/47.3[a]	9.3
2058	P(St-*co*-BMA)/DOP	50/50	77.5	9.5	12.6	7.7	13.6	3.4	7.3	2.1	8.5/42.0[a]	2.4
2051 (ref. [23])	P(St-*co*-BMA)/PSt	(62.5/25)/12.5	75.4	8.4	14.7	6.1	20.9	0.5	3.4	6.9	23.8/58.4[a]	17.2/65.7[a]
2052 (ref. [23])	[P(St-*co*-BMA)/PSt]/DOP	(62.5/25)/12.5	52.0	6.2	17.5	5.5	21.2	0.5	2.8	5.2	21.2/50.0[a]	17.3

SPG pore size 0.90 μm. DOP was added 5 wt % of monomer.
[a] Two separate T_g values were observed.

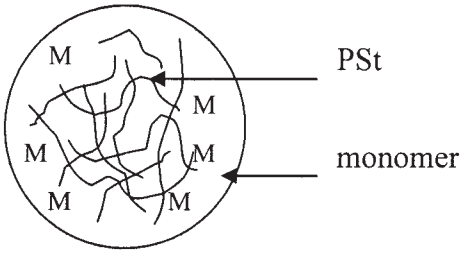

Figure 4 A schematic model for the phase separation of the poly(St-*co*-BMA)/PSt.

phases exist in monomer droplets, one is the PSt phase swollen with some monomers, and the other is the monomer-rich phase. The initiator molecules are located in majority in the monomer-rich phase. One can state that the polymerization dominantly takes place in the monomer-rich phase, and then the molecular weights of the copolymers formed are lower than the other runs without the addition of PSt.

The other possibility is derived from the gel effect theory, which refers to the autoacceleration of the polymerization rate due to the decrease in the termination rate constant when polymeric radicals are present in a viscous media. The termination reaction is influenced by the viscosity of the reaction medium from zero conversion. Soh et al.[28–31] considered that the termination reaction is diffusion controlled and that the diffusivity of macroradicals depends on chain length. It is rather difficult to prove the chain length dependence experimentally. The overall termination behavior is made up of a chain-length-dependent (translational diffusion) portion and a propagation-step-dependent portion. The latter is not related to chain length. When these dual mechanisms operate simultaneously, the overall termination rate constant chould be expressed as eq. (4)

$$k_t(y) = (k_t)_{\mathrm{tr}} + k_{\mathrm{tp}} \tag{4}$$

where $k_t(y)$ is the rate constant of the termination step, $(k_t)_{\mathrm{tr}}$ is the rate constant of translational step, and $k$tp is the rate constant of the propagation step. As described earlier, one can summarize that the mechanism of phase separation in composite particles is proposed based on the aforementioned thermodynamic effect and kinetic effect (behavior) as shown in Figure 5. A schematic model for the path of gel effect is shown in Figure 5(a). It was found that the polymer segments were short and easy to move in the dilute state. Then, the gel effect started to rise with the rise of viscosity inside the monomer droplets, with no hindrance of monomer diffusion but diffusion of polymeric chains were hindered. When the polymerization was completed, the steric hindrance of monomer diffusion was apparent.

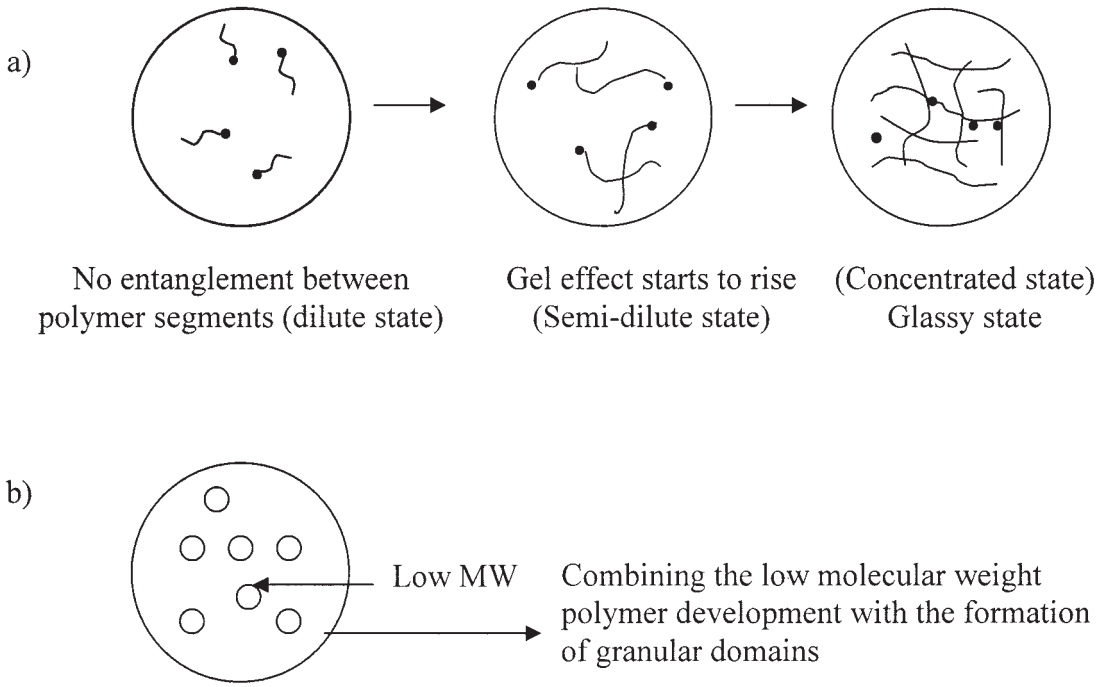

Figure 5 "Scaling model" demonstrated by Soh.[28–31] (a) A schematic model for the path of gel effect. (b) Illustration of morphological development.

Internal morphology of Poly(St-*co*-BMA)/PSt composite

For investigation of the mobility of the polymer segments in the composite particles during the polymerization, poly(St-*co*-BMA)/PSt composites were selected on the basis of morphology since the BMA monomer gave a lower T_g polymer. The formulations and results for each run are shown in Table III. It is known that the OsO_4 vapor stains PBMA better than it stains PSt. Most of the particles look ellipsoidal because of the compressive stress deformation caused by microtome. The darkly stained domains of the PBMA core grew inside and are embraced within the PSt shell as the core/shell-type polymer (shown in Figure 6(a)). In contrast, some of the particles revealed more homogeneity without showing much different contrasts of the stained areas. Thermodynamic considerations[32,33] were applied to the morphology of composite latex particles, which indicated that there was a more polar PBMA shell surrounding the hydrophobic PSt core. It yields a minimum interfacial tension of each phase, which controls primarily the arrangement of the polymer phases in latex particles. According to the thermodynamic theory that the morphology of the lowest change of Gibb's free energy (ΔG) will be dominant,[32,33] this suggests that the PBMA is concentrated in the shell region. When DOP was added in Run 2052, it was found that the PSt gained more compatibility between them by converting the small dispersed domains to become a large matrix, which resulted in a more perfect core–shell type. However, the phase separated domains of PSt still remained in the particles as

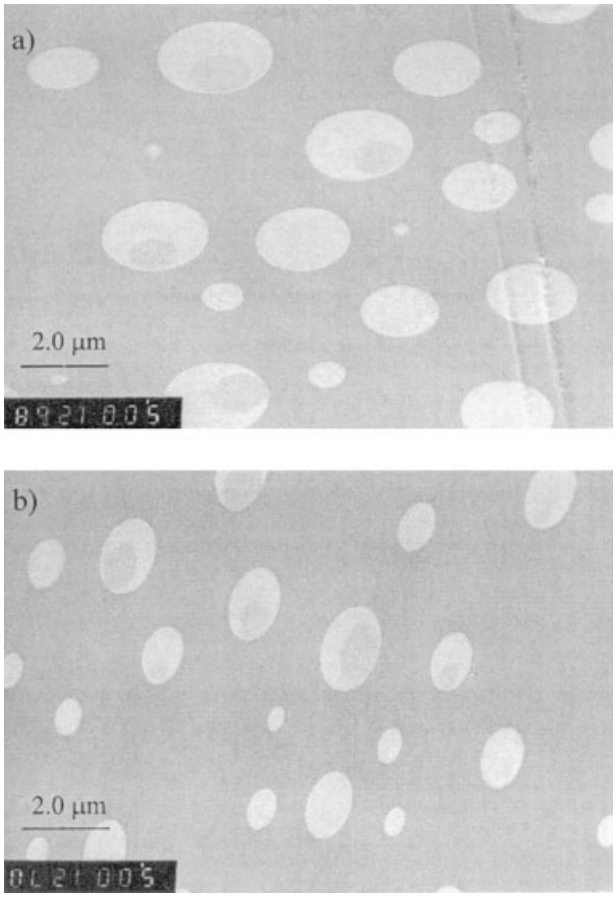

Figure 6 TEM photographs of microtomed, OsO_4-stained poly(St-*co*-BMA)/PSt composite particles: (a) St : BMA : PSt 62.5 : 25 : 12.5 (without DOP, Run 2051) and (b) St : BMA : PSt 62.5 : 25 : 12.5 (with DOP, Run 2052).

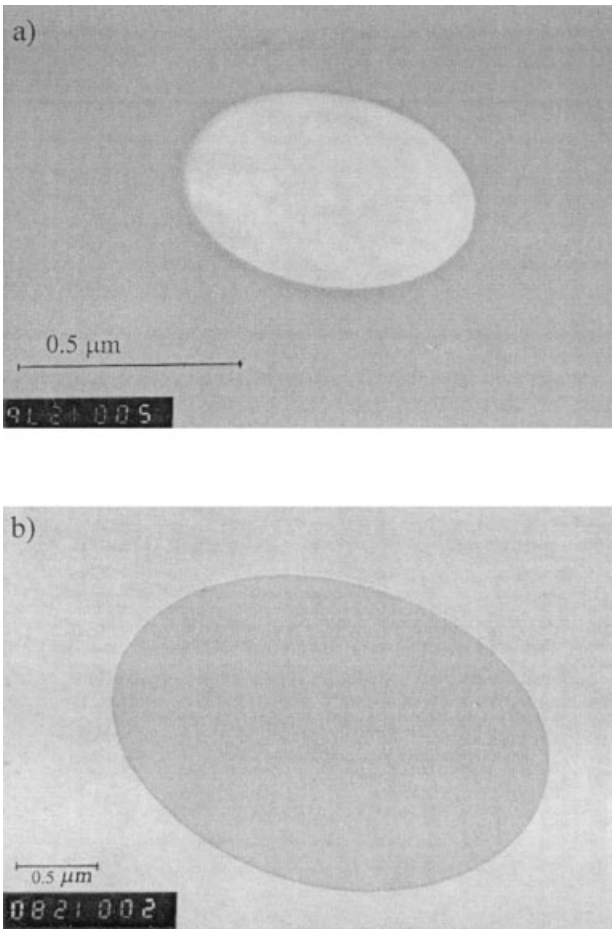

Figure 7 TEM photographs of microtomed, OsO_4-stained poly(St-*co*-BMA) copolymer particles: (a) St : BMA 75 : 25 (Run 2054) and (b) St : BMA 75 : 25 (with DOP 5 wt % of monomer, Run 2059).

shown in Figure 6(b), especially in the copolymer containing 5 wt % DOP. Upon the addition of DOP, the copolymer particles show both the core–shell morphology with the smooth interface between the stained-PBMA phase and unstained-PSt phase, and the homogeneous type. The reactivity ratio of BMA is relatively similar to that of styrene [r_1(St) = 0.52, r_2(BMA) = 0.47],[34] though the St–PSt fraction in the copolymer mixture is higher than BMA monomer. In any circumstance, the PSt portions were generated faster at the beginning of the polymerization to be the core polymer. The BMA-rich phase was then formed, which later became the shell to envelop the core-St structure. For example, poly(St-*co*-BMA) particles at the St-to-BMA ratio of 75 : 25, the TEM photographs in Figure 7(a,b) show the particles without any phase separation when the St-to-BMA composition was higher.

Effect of DOP on molecular weight and glass transition temperature of poly(St-*co*-BA) copolymer

The SPG membrane pore size 0.90 μm was used for the emulsification of St and BA monomer. The experimental results are shown in Table IV. The presence of the soft BA phase in the copolymer enhances synergistically the plasticizing effect of DOP. Since BA itself behaves like a plasticizing monomer, the expected single glass transition temperature was found in poly(St-*co*-BA) particles for both the clean and unclean samples (Run 2047). However, when PSt was added into the St-BA monomer mixture, the synthesized poly(St-*co*-BA)/PSt gave a single T_g in the unclean particles. In Contrast, the two separate T_gs were found in the clean particles. Likewise, the low number average molecular weight was also found as the aforementioned case of poly(St-*co*-BMA). One can mention that, the side chain of butyl acrylate is the key variable influencing the glass transition temperature because it is more flexible than that of BMA side chain.

The addition of PSt as the bulky molecule affected the molecular weight of polymer. Meanwhile, the influence of low molecular weight polymer was observed via the increasing viscosity of the initial dispersion phase. Since the bulky molecule of PSt retarded the propagation radicals in the propagation stage, a low molecular weight was yielded. The PSt increases the viscosity of the medium and can possibly retard the propagation rate of radicals of the comonomers. This will induce premature termination of the growing polymer chains to give low molecular weight polymers. Accordingly, the PSt domains gained increasing viscosity to the extent that the propagation of monomers was greatly hindered to give the short-chain polymer.

Internal morphology of poly(St-*co*-BA)/PSt composites

The polyacrylate polymer was preferentially stained with OsO_4. The cross section of copolymer composite revealed that the lightly-stained PSt granules were distributed over the whole area of the particle. Another phase separation of a salami-like morphology was also observed. The reactivity ratios of St (r_1) and BA (r_2) are 0.84 and 0.18,[25] respectively. A marked composition drift in the copolymer was observed as the reactivity ratios between St and BA monomers are largely different. Hence the monomer pair can then form a random copolymer because of the r_1r_2 value of 0.154. St monomer molecules were consumed faster at the beginning of the polymerization. Then, the BA-rich phase was subsequently produced, which surrounded the core-St domains. In comparison with poly(St-*co*-MA)/PSt as described earlier, the St–BA copolymer has an inverted morphology of the St–MA copolymer. Moreover, the BA-rich shell was also observed as shown in Figure 8(a,b). The resulting particle morphology indicated that a largely different reactivity ratio is then a key reason to govern the partic-

TABLE 4
Recipe and Results for Styrene and Butyl acrylate Copolymerization[23]

Run No.	Composition	Monomer composition (wt %)	Monomer conversion (%)	D_e (μm)	CV_e (%)	D_p (μm)	CV_p (%)	$\bar{M}_n$ ($\times 10^{-4}$)	$\bar{M}_w$ ($\times 10^{-4}$)	PDI	T_g (°C) clean	T_g (°C) unclean
2048	P(St-*co*-BA)	75/25	71.3	8.7	13.9	6.2	15.8	2.6	6.2	2.4	22.7/58[a]	17.4/51.6[a]
2047	P(St-*co*-BA)/DOP	75/25	65.1	8.1	15.1	6.5	16.3	2.1	4.9	2.3	40.2	16.8
2049	P(St-*co*-BA)/PSt	(62.5/25)/12.5	86.0	7.6	13.5	5.3	17.4	0.7	3.9	5.4	17.2/55[a]	18.8/52.0[a]
2050	P(St-*co*-BA)/PSt/DOP	(62.5/25)/12.5	67.9	6.8	21.7	5.2	23.3	0.6	3.7	5.9	22.2/53.3[a]	19.7

SPG pore size 0.90 μm, DOP concentration of 5 wt% was based on the monomer concentration.
[a] Two separate T_g values were observed, otherwise a single T_g.

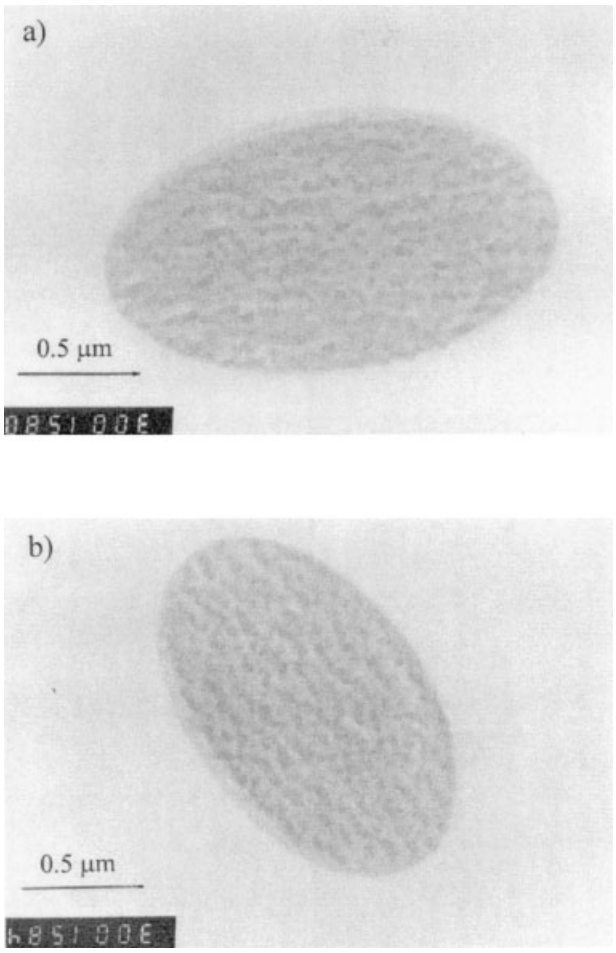

Figure 8 TEM photographs of microtomed, OsO_4-stained poly(St-*co*-BA)/PSt composite particles: (a) St : BA : PSt 62.5 : 25 : 12.5 (without DOP, Run 2049) and (b) St : BA : PSt 62.5 : 25 : 12.5 (with DOP, Run 2050).

ular morphology of the copolymer particles formed from the monomer pair.

CONCLUSIONS

The SPG emulsification and subsequent suspension polymerization were employed for the preparation of two-phase styrene–(meth) acrylate copolymer particles by incorporating DOP plasticizer. The effects of DOP plasticizer and PSt bulky molecules on the glass transition temperature (T_g) of the copolymer, and morphologies of the particles were investigated. The DOP molecules were well mixed with the monomers in the initial stage of emulsification and significantly decreased the polymer' T_g. The contribution of DOP to the PSt-based particles is to significantly enhance the mobility of the PSt backbone, and thus decreases T_g values of the copolymers. Fairly uniform poly(St-*co*-MA) microspheres were obtained. The morphology of the particles could be controlled by adding DOP or varying the PSt/PMA ratio. When PSt was added, the core–shell morphology dispersed as mi-

crodomains were obtained in the absence of DOP. The slightly nonpolar DOP preferentially plasticized the matrix phase of both the hard PSt and soft (meth)acrylate phases. Upon washing the polymer particles with methanol, DOP in the polymers was washed out, and two separate T_g peaks were observed. Microphase separation was found when the monomer droplets were formed at a later stage in the emulsification process. Small particles with a broad molecular weight distribution were then produced. Moreover, the addition of PSt induced a high viscosity at the dispersion phase. The molecular weight slightly increased with increasing St/PSt concentration. The multiple-phase separation of the St-rich phase and PMA domains observed by TEM was caused by the composition drift because the MA reactivity ratio is greater than that of St. The addition of DOP revealed more compatibility between the hard-St and soft-MA moieties than that without DOP.

For Poly(St-*co*-BMA) composite in the presence of 5 wt % of DOP, the unclean particles gave a single T_g, even though the DOP could be washed out from the particles by methanol; the existing of BMA in copolymer could also function as an internal plasticizer within its own copolymer. The addition of PSt-rich phase before polymerization produced smooth surfaces of particles. A core–shell-type polymer resulting from the phase separation between PSt and PBMA-rich phase was revealed by TEM in which the PSt shell embraced the hydrophobic PBMA-rich core.

The thermal behavior of poly(St-*co*-BA) revealed that BA itself also behaves like a plasticizing monomer as indicated by the single T_g found in all compositions of poly(St-*co*-BA) particles for both clean and unclean samples. It implies that both internal and external plasticizers are compatible. However, when PSt was dissolved in the St–BA monomer mixture, poly(St-*co*-BA)/PSt gave only a single T_g in the unclean particles. For the clean particles, two separate T_g values were found. The TEM photographs of the cross-section of the copolymer composites revealed that the lightly stained PSt granules were spread over the whole area of the particle. Another type of the phase separation with a salami-like morphology was also disclosed. The reactivity ratio was claimed to be the main factor, which induced the phase separation because the St monomer molecules were consumed faster at the beginning of the polymerization.

The influence of DOP on the T_g of copolymer and phase separation was revealed. The copolymers with the lower T_g were obtained. The copolymer comprising the low T_g values of alkyl methacrylate monomers of MA, BMA, and BA were successfully prepared. Effects of the DOP plasticizer on T_g of poly(St-*co*-MA), poly(St-*co*-BMA), and poly(St-*co*-BA) particles demonstrate that the incompatibility between DOP and high-T_g PSt may provide a phase separation resulting in two separate T_g values. The different values of lower T_g and higher T_g of the copolymer were found in the following sequence: poly(St-*co*-MA) > poly(St-*co*-BMA) > poly(St-*co*-BA). The ultimately interesting point is that poly(St-*co*-BA) incorporating DOP exhibited only one T_g value. It indirectly implies that both internal and external plasticizers are compatible with each other.

The authors would like to express their sincere appreciation to the Golden Jubilee Program of the Thailand Research Fund (TRF) for providing a scholarship through the Contract Number 2.M.CU/42/E.1 and to the Bio-Applications and Systems Engineering, Tokyo University of Agriculture and Technology, Tokyo, Japan for providing research facilities to the first author to carry out this research.

References

1. Vanderhoff, J. W.; Sheu, H. R.; El-Aasser, M. S. In Scientific Methods for the Study of Polymer Colloids and Their Applications; Candau, F.; Ottewill, R. H., Eds.; Kluwer: The Netherlands, 1990; p 529.
2. Ugelstad, J.; Kaggerud, K. H.; Hansen, F. K.; Berge, A. Makromol Chem 1979, 180, 737.
3. Ugelstad, J.; Mørk, P. C.; Mfutakamba, H. R.; Soleimany, E.; Nordhuus, I.; Schmidt, R.; Berge, A.; Ellingsen, T.; Aune, O.; Nustad, K. In Science and Technology of Polymer Colloids, Vol. 1; Poehlein, G. W.; Ottewill, R. H.; Goodwin, J. W., Eds.; NATO ASI Series E, Applied Science, No. 67; Martinus Nijhoff: Boston, 1983; p 51.
4. He, Y.; Daniels, E. S.; Klein, A.; El-Aasser, M. S. J Appl Polym Sci 1997, 64, 1143.
5. Park, J. G.; Kim, J. Y.; Suh, K. D. J Appl Polym Sci 1998, 69, 2291.
6. Okubo, M.; Takekoh, R.; Izumi, J.; Yamashita, T. Colloid Polym Sci 1999, 277, 972.
7. Hatate, Y.; Ohta, H.; Uemura, Y.; Ijichi, K.; Yoshizawa, H. J Appl Polym Sci 1997, 64, 1107.
8. Omi, S.; Kaneko, K.; Nakayama, A.; Katami, K.; Taguchi, T.; Iso, M.; Nagai, M.; Ma, G. H. J Appl Polym Sci 1997, 65, 2655.
9. Kandori, K.; Kishi, K.; Ishikawa, T. Colloids Surf 1992, 62, 259.
10. Nakashima, T.; Shimizu, M.; Kukizaki, M. Key Eng Mater 1991, 61–62, 513.
11. Nakashima, T.; Shimizu, M.; Kukizaki, M. Membrane Emulsification Operation Manual; Deparment of Chemistry, Industrial Research Institute of Miyazaki Prefecture: Miyazaki, Japan, 1991; p 1.
12. Lee, H. J.; Kim, J. H. Membrane J 1996, 6, 166.
13. Kandori, K.; Kishi, K.; Ishikawa, T. Colloids Surf 1991, 55, 73.
14. Baba, Y.; Nakamura, S.; Fujimoto, K.; Ohe, K.; Shimizu, M.; Nakashima, T. http://www.cape.canterbury.ac.nz/apcche Proceedings/APCCHE/data/434rev.pdf; Dated 2003.
15. Omi, S.; Katami, K.; Yamamoto, A.; Iso, M. J Appl Polym Sci 1994, 51, 1.
16. Omi, S.; Katami, K.; Taguchi, T.; Kaneko, K.; Iso, M. J Appl Polym Sci 1995, 57, 1013.
17. Omi, S.; Katami, K.; Taguchi, T.; Nagai, M.; Ma, G. H. J Appl Polym Sci 1997, 63, 931.
18. Hatate, Y.; Uemura, Y.; Ijichi, K.; Kato, Y.; Hano, T.; Baba, Y.; Kawano, Y. J Chem Eng Jpn (in Japanese) 1995, 28, 656.
19. Hosoya, K.; Ohta, H.; Yoshizako, K.; Kimata, K.; Ikegami, T.; Tanaka, N. J Chromatogr A 1999, 853, 11.
20. Ha, Y. K.; Song, H. S.; Lee, H. J.; Kim, J. H. Colloids Surf A: Physicochem Eng Aspect 1999, 162, 289.
21. Kiatkamjornwong, S.; Nuisin, R.; Ma, G. H.; Omi, S. Chin J Polym Sci 2000, 18, 309.

22. Nuisin, R.; Ma, G. H.; Omi, S.; Kiatkamjornwong, S. J Appl Polym Sci 2000, 77, 1013.
23. Nuisin, R.; Omi, S.; Kiatkamjornwong, S. J Appl Polym Sci 2003, 90, 3037.
24. Omi, S.; Senba, T.; Nagai, M.; Ma, G. H. J Appl Polym Sci 2001, 79, 2200.
25. Brandup, J.; Immergut, E. H.; Gruke, E. A., Eds.; Polymer Handbook, 4th ed.; Wiley: New York, 1999; p VII/250.
26. Schulze, U.; Pompe, G.; Meyer, E.; Janke, A.; Pionteck, J.; Fiedlerová, A.; Borsig, E. Polymer 1995, 36, 3393.
27. Vitali, R.; Montani, E. Polymer 1980, 21, 1220.
28. Soh, S. K.; Sundberg, D. C. J Polym Sci Polym Chem Ed 1982, 20, 1299.
29. Soh, S. K.; Sundberg, D. C. J Polym Sci Polym Chem Ed 1982, 20, 1315.
30. Soh, S. K.; Sundberg, D. C. J Polym Sci Polym Chem Ed 1982, 20, 1231.
31. Soh, S. K.; Sundberg, D. C. J Polym Sci Polym Chem Ed 1982, 20, 1345.
32. Sundberg, D. C.; Casassa, A. P.; Pantazopoulos, J.; Muscato, M. R.; Kronberg, B.; Berg, J. J Appl Polym Sci 1990, 41, 1425.
33. Chen, Y. C.; Dimonie, V.; El-Aasser, M. S. J Appl Polym Sci 1991, 42, 1049.
34. Brandup, J.; Immergut, E. H.; Gruke, E. A., Eds.; Polymer Handbook, 4th ed.; Wiley: New York, 1999; p VII/259.